

Irreversible magnetization in thin $YBCO$ films rotated in external magnetic field*

R. Prozorov, A. Poddar, E. Sheriff, A. Shaulov, Y. Yeshurun
Institute for Superconductivity, Physics Department, Bar-Ilan University,
52900 Ramat-Gan, Israel

(Received: (26-Feb-1996) Accepted: (17-April-1996))

Abstract

The magnetization M of a thin $YBa_2Cu_3O_{7-\delta}$ film is measured as a function of the angle θ between the applied field H and the c -axis. For fields above the first critical field, but below the Bean's field for first penetration H^* , $M(\theta)$ is symmetric with respect to $\theta = \pi$ and the magnetization curves for forward and backward rotation coincide. For $H > H^*$ the curves are asymmetric and they do not coincide. These phenomena have a simple explanation in the framework of the Bean critical state model.

PACs: 74.60.-w, 74.25.Ha, 74.60.Ec, 74.60.Ge, 74.60.Jg

Typeset using REVTeX

*Accepted in *Physica C*

I. INTRODUCTION

The anisotropic properties of high-temperature superconductors have motivated measurements of their magnetization M as a function of the angle θ between the external DC magnetic field H and one of the principal axis of the superconductor. Such experiments may supply ample information regarding the superconducting properties and they were used for studies of the 3D anisotropic Ginzburg-Landau theory in single $YBa_2Cu_3O_{7-\delta}$ crystal [1], pinning strength distribution in polycrystalline materials [2–6], intrinsic anisotropy [7,8] and interaction of vortices with pinning sites and external magnetic fields [3,6,9]. The conclusions in these works were drawn from the peculiarities observed in rotation curves at different ambient conditions. Thus, for example, it was found that in relatively high fields, well above the lower critical field H_{c1} , the $M(\theta)$ curves in forward and backward rotations do not coincide [3,7–9]. This was taken as an evidence that the magnetic moment rotates frictionally, lagging behind the sample, due to the interaction of vortices with the external field, thus exhibiting irreversible (hysteretic) behavior and an apparent phase shift between the two magnetization curves. Such a phase shift was not observed in lower fields, where the two curves were found to coincide and it has been believed to indicate that the sample is in a pure reversible (or Meissner) state. The main purpose of this work is to demonstrate that the forward and backward rotation curves coincide even in the irreversible state, for fields between H_{c1} and H^* , and that the observed hysteretic behavior in higher fields may find a simple explanation within the framework of the Bean critical state model [10].

We present here measurements of the angular dependence of the magnetization curves $M(\theta)$ of a thin $YBa_2Cu_3O_{7-\delta}$ (YBCO) film. As demonstrated below, in thin films we can safely neglect the in-plane component of magnetic moment. Therefore, the results of rotational experiments are clear and much easier to interpret. We find that for fields *below* the Bean's first penetration field H^* , $M(\theta)$ is symmetric with respect to $\theta = \pi$ and the rotation curves for forward and backward rotation coincide (see also [7]). For $H > H^*$ the curves are asymmetric and they do not coincide. Moreover, the backward curve is a mirror

image (with respect to $\theta = \pi$) of the forward one.

The basic idea of our explanation is that in order to understand the variation of M during rotation in a system with isotropic pinning one has to consider separately the variation of its components along the c - axis (M_c) and the ab - plane (M_{ab}). This leads to a consideration of the projections of the applied field on the c - axis (H_c) and the ab - plane (H_{ab}), respectively. The effective field H_c cycles during the rotation between $\pm H$ and the calculation of $M(\theta)$ is thus analogous to the calculation of $M(H)$. We demonstrate the validity of this concept by comparing direct measurements of $M(H)$ and $M(\theta)$. We stress, that this claim is true only if a sample does not have any induced anisotropy of pinning, e.g., twin boundaries or columnar defects. Although, the analysis below can be easily extended to account for more general, anisotropic case.

Many authors pointed out the importance of the geometry for proper analysis of the rotation experiment. In previous works this was limited to a consideration of the demagnetization in a reversible state [7,11], i.e. to the actual field on the sample edge which varies during rotation because of demagnetization. Maintaining this point, we further show how demagnetization affects the rotation curves in an irreversible state. In particular, we find that the interval of angles for which the sample undergoes remagnetization shrinks dramatically as a result of a flat geometry. This results in sharp changes in $M(\theta)$.

II. EXPERIMENTAL

A thin *YBCO* film of thickness $\simeq 1000$ Å and lateral dimensions of 5×5 mm² was laser ablated on a *SrTiO*₃ substrate [12]. The film is c - oriented, so that the c - axis points in a normal to a film surface direction with angular dispersion less than 2° and the ab - plane coincides with the film plane. For the rotation magnetic measurements we used an "Oxford Instruments" Vibrating Sample Magnetometer (*VSM*) that enables sample rotation relative to an external magnetic field with a 1° precision. The rotation axis is always perpendicular to the c - axis. Samples were zero field cooled down to the desired temperature whence

an external magnetic field H was turned on. The component of the magnetic moment M_H along the external field direction was then measured while the sample was rotated one full turn ("forward rotation") and then back ("backward rotation"). The initial field application was always along the c -axis. We find that turning on the external field at other angles does not yield any new information, since the rotation curve becomes independent of this angle after one full rotation - (see also [8]).

Throughout this paper M_H is the magnetic moment component along the direction of the external field H . We recall that in a VSM, as well as in most other magnetometers, M_H is the *measured* component of the total magnetic moment. In Fig. 1 we sketch the relevant vectors and angles.

III. RESULTS

The symbols in Fig. 2 present the measured angular dependence of the zero-field-cooled (ZFC) magnetization, $M_H(\theta)$, for the *YBCO* film at different values of H and at 20 *K*. (At this temperature, the apparent $H_{c1} \approx 50$ *G*, and $H^* = 380$ *G*, as determined from direct "static" $M(H)$ measurements). The rotation curves are symmetric with respect to $\theta = \pi$, in spite of the fact that the applied fields are larger than H_{c1} . Also, we find that the magnetization curves for forward and backward rotation coincide. This implies that such reversibility with respect to direction of rotation is not indicative of the *true* magnetic reversibility. Note, that curve for $H = 400$ *G* $> H^*$ is shown only for comparison.

Figures 3-5 exhibit $M_H(\theta)$ data collected at 20 *K* for fields above H^* . Fig. 3 demonstrates that as a result of an increase in the external field, the rotation curves become gradually more and more asymmetrical with respect to $\theta = \pi$. For field slightly larger than H^* the forward and backward rotation curves look harmonically, but with some phase shift, see Fig. 4. High - field measurements, shown in Fig. 5 demonstrate that the backward rotation curve is a mirror image of the forward one with respect to $\theta = \pi$. Therefore, we conclude that the observed asymmetry do not imply a phase shift, but a true magnetic hysteresis with respect

to rotation, which means a reverse of the magnetic moment when the direction of rotation is reversed. We shall return to this point in the analysis.

We complete the experimental picture by presenting in Fig. 6 the rotation curves at $H = 1.5 \text{ Tesla}$ measured at different temperatures. The width and height of steep change in a magnetic moment shrinks as the temperature increases and, in some sense, the increase of temperature is analogous to the increase of magnetic field. As we show below, all these features find natural explanation in a framework of the Bean model.

IV. ANALYSIS

We present a model that takes into account the variation of the *effective* field along the sample sides during rotation. Specifically, during a rotation cycle, H_c , the field component along the c -axis, oscillates as $H_c = H \cos(\theta)$. This leads to a variation of M_c similar to that in a standard magnetization loop, where the magnetization M_c is measured as a function of the external magnetic field between $-H$ to $+H$ at $\theta = 0$. Therefore, in order to analyze a rotation experiment one has to consider the *effective* applied field H_c along the c - axis, and not the actual applied field H . This approach leads directly to the consideration of the two field regimes: (a) Moderate fields: $H \leq H^*$, where the sample space is only partially occupied by magnetic flux and (b) High fields: $H \geq H^*$, where flux occupies the entire sample space. These two regimes are discussed below. We note that for fields below H_{c1} the correct analyses of the data was given previously in a number of reports, e.g. [7,11].

In order to elucidate the relative importance of each component of the applied field we start by calculating the components of the magnetization along the c - axis, M_c , and in the ab - plane, M_{ab} . For an estimate of the relative contribution of M_c and M_{ab} to the total magnetic moment we apply the Bean model to a finite slab as, for example, in Refs. [10,13,14]. (The validity of this approach was examined experimentally on both films [13] and crystals [14]). Then (by taking $t \leq L \leq d$, see Fig. 1) one obtains:

$$\begin{cases} |M_c| \approx \frac{|J_c^a|}{40} L \left(1 - \frac{L}{3d}\right) \equiv \frac{H_c^*}{2} \\ |M_{ab}| \approx \frac{|J_c^c|}{40} t \left(1 - \frac{t}{3L}\right) \equiv \frac{H_{ab}^*}{2} \end{cases} \implies$$

$$\beta \equiv \left| \frac{M_c}{M_{ab}} \right| \approx \frac{H_c^*}{H_{ab}^*} = \frac{|J_c^{ab}|}{|J_c^c|} \frac{L}{t} \frac{\left(1 - \frac{L}{3d}\right)}{\left(1 - \frac{t}{3L}\right)} \quad (1)$$

where the magnetization is in emu/cc , current densities are in A/cm^2 and lengths are in cm . H_c^* and H_{ab}^* are the effective penetration fields along the c -axis and the ab -plane, respectively. $J_c^{ab}(H_c)$ and $J_c^c(H_{ab})$ are the persistent current densities flowing in and out of the ab -plane, respectively. For our sample (typical for thin films) $d = L = 0.5 \text{ cm}$, $t = 10^{-5} \text{ cm}$, the above ratio becomes approximately $\beta \approx 3 \cdot 10^4 \frac{|J_c^{ab}|}{|J_c^c|}$. This shows that in the case of thin film we can safely omit the in-plane component of the magnetic moment M_{ab} and in-plane component of the applied field - H_{ab} . We note that this simplification is not crucial for the analysis. Moreover, one ought to include both components of magnetic moment and field analyzing data for thick samples. This can be easily done using the same approach, as we undertake below.

As it is stated above, the *measured* magnetization, M_H , in a VSM, as well as in many other techniques, is the component of the magnetization along the external field. It is convenient to express M_H as $M_H(\theta) = \left| \overrightarrow{M}(\theta) \right| \cos \theta = M_c(\theta) \cos \theta + M_{ab}(\theta) \sin \theta$. For thin films, as shown above, one may safely rewrite this equation as $M_H(\theta) = M_c(\theta) \cos \theta$. Below we use $H^* = H_c^*$.

It should be noted, that for a sake of clarity, the analysis below is based on the Bean model for an infinite slab. Whereas in a fully magnetized state the magnetization for a thin sample and for an infinite slab is the same and given by Eq. 1, the remagnetization process is quite different [15]. Nevertheless, we use the simple Bean model first, in order to demonstrate a general approach to the problem avoiding an unnecessary complications of the analysis. As we show latter (Fig. 7) we could even use a linear approximation for a remagnetization stage.

Partial magnetization ($H \leq H^$)*

Utilizing the parameter $x = 1 - \cos(\theta)$ one may express the difference between the external magnetic field H and its projection on the c -axis during rotation, as $\Delta H = Hx$. In the following we describe a ZFC experiment and consider *forward* rotation only. The *backward* rotation may be obtained from the formulae below by substituting $\theta_{back} = 2\pi - \theta$. The curve obtained by such a substitution *coincides* with the forward curve.

In the framework of the Bean model we get for the projection of the total moment along the c -axis:

$$M_c = -\frac{H^2}{8H^*} (x^2 + 2x - 4) - H(1 - x). \quad (2)$$

Note that for $x = 0$ we recover the Bean result for partial magnetization. The component M_c varies continuously with θ in a whole interval of angles implying that the magnetic flux profile inside the sample changes for any change in θ . In the following we refer as 'remagnetization' to the parts of the process for which the profile is changing.

Eq. 2, when expressed in terms of θ , yields, for the measured component of the total moment along the direction of the external magnetic field:

$$M_H = H \cos(\theta) \left\{ \frac{H}{8H^*} \sin^2(\theta) - \left(1 - \frac{H}{2H^*}\right) \cos(\theta) \right\}. \quad (3)$$

Apparently, the magnetization curves for *backward* and *forward* rotations are symmetric with respect to $\theta = \pi$ and therefore they *coincide*. In other words, reversibility with respect to the direction of rotation does not imply a "true" magnetic reversibility which is expected either in the Meissner state or in the unpinned state.

The magnetic moment along the c -axis reaches a maximum value of

$$|M_c|_{\max} = |M_H|_{\max} = H_{ab} \left(1 - \frac{H}{2H^*}\right) \quad (4)$$

at $x = 0$ and 2, (i.e. $\theta = 0, \pi$ and 2π).

Fig. 2 shows a good agreement between Eq. 3 and the experiment. In this figure the symbols represent the experimental data whereas the solid lines are fits to Eq. 3 with a

single parameter $H^* \approx 380 \text{ G}$, for all curves. The value of H^* was determined from a fit of the maximum value of M_H to Eq. 4 (inset to Fig. 2) and was verified through independent measurements of standard magnetization loops in that sample.

Another implication of Eq. 3 is that as long as the applied field H is smaller than or equal to H^* , the component M_H of the total magnetic moment is less than (or equal to) zero in the whole angular range. We show below that for $H > H^*$, M_H becomes positive at certain angles. This crossover from negative to positive values of M_H may serve as a sensitive tool for experimental determination of H^* . In Fig. 2 this crossover occurs at $H = H^* \approx 380 \text{ G}$. An additional line at $H = 400 \text{ G} > H^*$ is shown for comparison.

Full magnetization ($H \geq H^$)*

When the applied field is larger than H^* magnetic flux penetrates the entire sample space. In this case, the projection of the magnetic moment along the c -axis in the interval $x = [0, 2]$ (i.e. $\theta = [0, \pi]$) according to the Bean model is:

$$M_c = \begin{cases} \frac{3}{4}Hx - \frac{1}{8}\frac{H^2}{H^*}x^2 - \frac{H^*}{2} & x \leq 2\frac{H^*}{H} \\ \frac{H^*}{2} & x \geq 2\frac{H^*}{H} \end{cases} \quad (5)$$

Again, we note that for $x = 0$ we recover the Bean results for full penetration $|M_c| = H^*/2$. For $x \geq 2\frac{H^*}{H}$ the magnetization is constant as predicted by Bean for $H > H^*$. Only for $x \leq 2\frac{H^*}{H}$ we get a non trivial result which reflects the fact that the effective field is being reversed. Thus, the remagnetization process is limited now to $x \leq 2\frac{H^*}{H}$ and it is completed when the moment reverses its sign (i.e. changes from $-\frac{H^*}{2}$ to $+\frac{H^*}{2}$).

The measured component of the magnetic moment along the direction of the external field may be determined from Eq. 5 by substituting $x = 1 - \cos(\theta)$:

$$M_H = \begin{cases} \frac{H}{8} \cos(\theta) \left(-\frac{H}{H^*} (1 + \cos(\theta))^2 \right) + 2 \left(\frac{H}{H^*} - 3 \right) \cos(\theta) + 6 - \frac{4H^*}{H} & \theta \leq \theta_r \\ \frac{H^*}{2} \cos(\theta) & \theta \geq \theta_r \end{cases} \quad (6)$$

where, $\theta_r = \arccos(1 - 2H^*/H) \leq \pi$ is the angle at which the remagnetization process is completed.

An interesting implication of Eq. 6 is that for $H > H^*$ the resulting magnetization versus angle curves become *asymmetric* with respect to $\theta = \pi$. Hence, the *backward* rotation curve *does not coincide* with the *forward* rotation curve. We thus assert that generally, a *forward* and a *backward* magnetization versus angle curves would not coincide if $H > H^*$ and not, as previously believed, when $H > H_{c1}$. Also, the backward curve is a mirror image of a forward one with respect to $\theta = \pi$.

The solid lines in Fig. 6 are fits to Eq.6. The sharp change in M_H indicates a reversal of the magnetic moment ($\Delta M = H^*$) within a narrow angular interval. We explain this feature in the next section by considering the demagnetization effects.

Demagnetization effects

One may regard demagnetization effects as a renormalization of the applied magnetic field. In fact, to be more precise, the applied field H in the above formulae should be replaced with the actual magnetic field intensity at the specimen edges, which is in the simplest form: $H^{eff} = H + \gamma H^*$, where γ is a dimensionless parameter accounting for demagnetization. (Note the difference with the usual notion for a demagnetization correction for reversible state).

The remagnetization region, as described above, occurs when the projection of the applied magnetic field H_c changes sign. In standard magnetization - loop measurements it happens twice in each full loop and it was analyzed previously, see, e.g., [10,16]. One may therefore refer to the analysis of a standard magnetization measurements in order to gain understanding with regard to its effects within rotation experiments. The magnetic field interval, within which the remagnetization occurs for infinite slab is $\Delta H = 2H^*$ for infinite slab. However, for finite sample, one must bear in mind that when referring to this interval one actually refers to the *effective* magnetic field on the sample edges $\Delta H^{eff} = 2H^* = \Delta H + \gamma H^*$, or $\Delta H = (2 - \gamma) H^*$. Thus, since the demagnetization effects lead to an increase of H^{eff} with a decrease of sample thickness, the applied external field interval for remagnetization shrinks for thinner samples [17]. Demagnetization effects therefore change the angular in-

terval for remagnetization to complete: $\theta_r^{eff} = \arccos(1 - 2H^*/H^{eff})$. The total change in magnetic moment retains its original value $\Delta M = H^*$. This conclusion is in a good agreement with presented data on thin film, where we find a very narrow angular interval for remagnetization, within which the moment of a large magnitude changes sign.

Finally, in order to verify experimentally our assumption about the similarity between the standard magnetization loops and the rotation experiment we show in Fig. 7 a standard $M(H)$ loop (solid line) measured with the applied field along the c - axis, along with a "converted" $M_c(H_c)$ loop, i.e. $M_c = M_H/\cos(\theta)$ versus $H_c = H\cos(\theta)$. The remarkable similarity between the two curves supports our approach in explaining the data.

As we noted above, such correspondence of loops is possible only, if a sample does not have induced extrinsic anisotropy. In the case of anisotropic pinning, in a first approximation in the expressions above, the characteristic penetration field should be replaced by $H^*(\theta)$. More rigorous treatment requires exact analysis of the magnetic flux evolution in the sample during rotation with subsequent calculation of $M(\theta)$.

V. SUMMARY AND CONCLUSIONS

Detailed analysis based on the Bean model of the irreversible magnetization of a rotating type-II superconductor is presented. We assert that during rotation, the magnetic moment changes its sign with respect to the c -axis. This remagnetization happens within a finite angular interval, yielding an asymmetric rotation curve. All main features observed in the experiment are explained from this point of view. It is shown that demagnetization does not change the functional dependence of M_H vs. angle curve, however it does affect it by shrinking the angular interval within which the remagnetization occurs.

Acknowledgments: We thank Gad Koren for providing us with $YBCO$ thin films. This research was supported in part by the Israeli Science Foundation administered by the Israeli Academy of Science and Humanities and, in part, by the Heinrich Hertz Minerva Center for High Temperature Superconductivity. Y. Y. acknowledges a support from the DG

XII, Commission of the European Communities and the Israeli Ministry of Science and the Arts (MOSA). A. S. acknowledges a support from the Israeli-France cooperation program AFIRST.

REFERENCES

- [1] P. Pugnatz, G. Fillion, S. Khene, H. Noel, P. Schuster, B. Barbara, *Physica B* **194-196** (1994) 2055.
- [2] A. Mumtaz, H. Athar, S. K. Hasanain, J. A. Khan, *Solid State Comm.* **79** (1991) 60.
- [3] H. P. Goeckner, J. S. Kouvel, *J. Appl. Phys.* **73** (1993) 5860.
- [4] L. Liu, J. S. Kouvel, T. O. Brun, *J. Appl. Phys.* **67** (1990) 4527; L. Liu, J. S. Kouvel, T. O. Brun, *J. Appl. Phys.* **70** (1991) 5733; L. Liu, J. S. Kouvel, T. O. Brun, *Phys. Rev. B* **46** (1992) 14113 .
- [5] G. H. Khosa, S. H. Hasanain, A. N. Kayani, *Supercond. Sci. Technol.* **8** (1995) 534.
- [6] M. K. Hasan, S. J. Park, J. S. Kouvel, *Physica C* **254** (1995) 323.
- [7] U. Yaron, I. Felner and Y. Yeshurun, *Phys. Rev. B* **44** (1991) 12531; I. Felner, U. Yaron, Y. Yeshurun, G. V. Chandrashekar, F. Holtzberg, *Phys. Rev. B* **40** (1989) 5239; Y. Wolfus, Y. Yeshurun, I. Felner, *Phys. Rev. B* **37** (1988) 3667.
- [8] S. K. Hasanain, Ghulam Husain Khosa, M. K. Iqbal and N. A. Khan. *Supercon. Sci. Technol.* **6** (1993) 691.
- [9] M. Kim, S. Yu, S. Oh, *Appl. Phys. Lett.* **63** (1993) 2423.
- [10] C. P. Bean, *Phys. Rev. Lett.* **8** (1962) 250; C. P. Bean, *Rev. Mod. Phys.* **36** (1964) 31.
- [11] S. Kolesnik, T. Skośkiewicz, J. Igalson, *Phys. Rev. B* **43** (1991) 13679.
- [12] G. Koren, E. Polturak, B. Fisher, D. Cohen, G. Kimel, *Appl. Phys. Lett.* **50** (1988) 2330.
- [13] F. Hellman, E. M. Gyorgy, R. C. Dynes, *Phys. Rev. Lett.* **68** (1992) 867.
- [14] Y. Yeshurun, M. W. McElfresh, A. P. Malozemoff, J. Haghurst-Trewhella, J. Manhart, F. Holtzberg, G. V. Chandrasekar, *Phys. Rev. B* **42** (1990) 6322.

- [15] E. H. Brandt, M. I. Indenbom, Phys. Rev. B **48** (1993) 12893; E. Zeldov, J. R. Clem, M. McElfresh, M. Darwin, Phys. Rev. B **49** (1994) 9802.
- [16] E. H. Brandt, Rep. Prog. Phys. **58** (1995) 1465.
- [17] M. Oussena, P. A. J. de Groot, R. Gagnon, L. Taillefer, Alpbach'94 (1994) 137.

FIGURES

FIG. 1. Geometrical aspects of the experiment. The rotation axis is always perpendicular to the c -axis.

FIG. 2. Angular dependence of the ZFC magnetization (M_H) at 20 K for *YBCO* film at different values of H . Symbols are experimental points and solid lines are calculated from Eq. 3. *Inset* shows the variation of maximum moment $|M_H|_{\max}$ with H . Solid line is a fit to Eq. 4.

FIG. 3. Angular dependence of the ZFC magnetization (M_H) at 20 K for *YBCO* film at different values of $H > H^*$.

FIG. 4. Forward and backward rotation curves measured at 20 K for *YBCO* film at $H = 400$ G.

FIG. 5. Forward and backward rotation curves measured at 20 K for *YBCO* film at $H = 15000$ G.

FIG. 6. Angular dependence of the magnetisation M_H at different temperatures for *YBCO* thin film, $H = 15000$ G.

FIG. 7. Comparison of the standard magnetization loop $M(H)$ (solid line) with the loop, constructed from the rotation experiment (open circles) as described in the text.

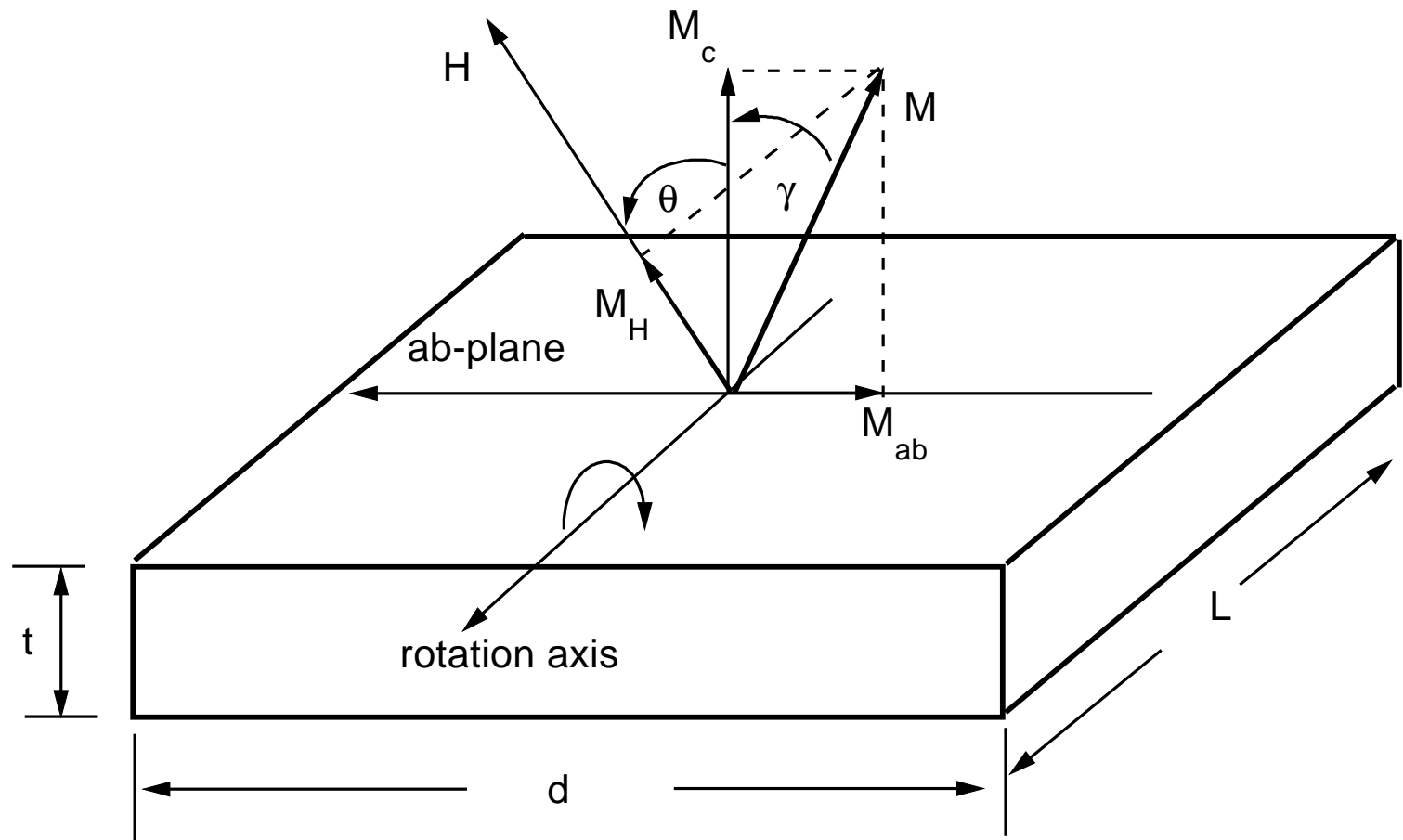


Fig.1

(Prozorov et al.)

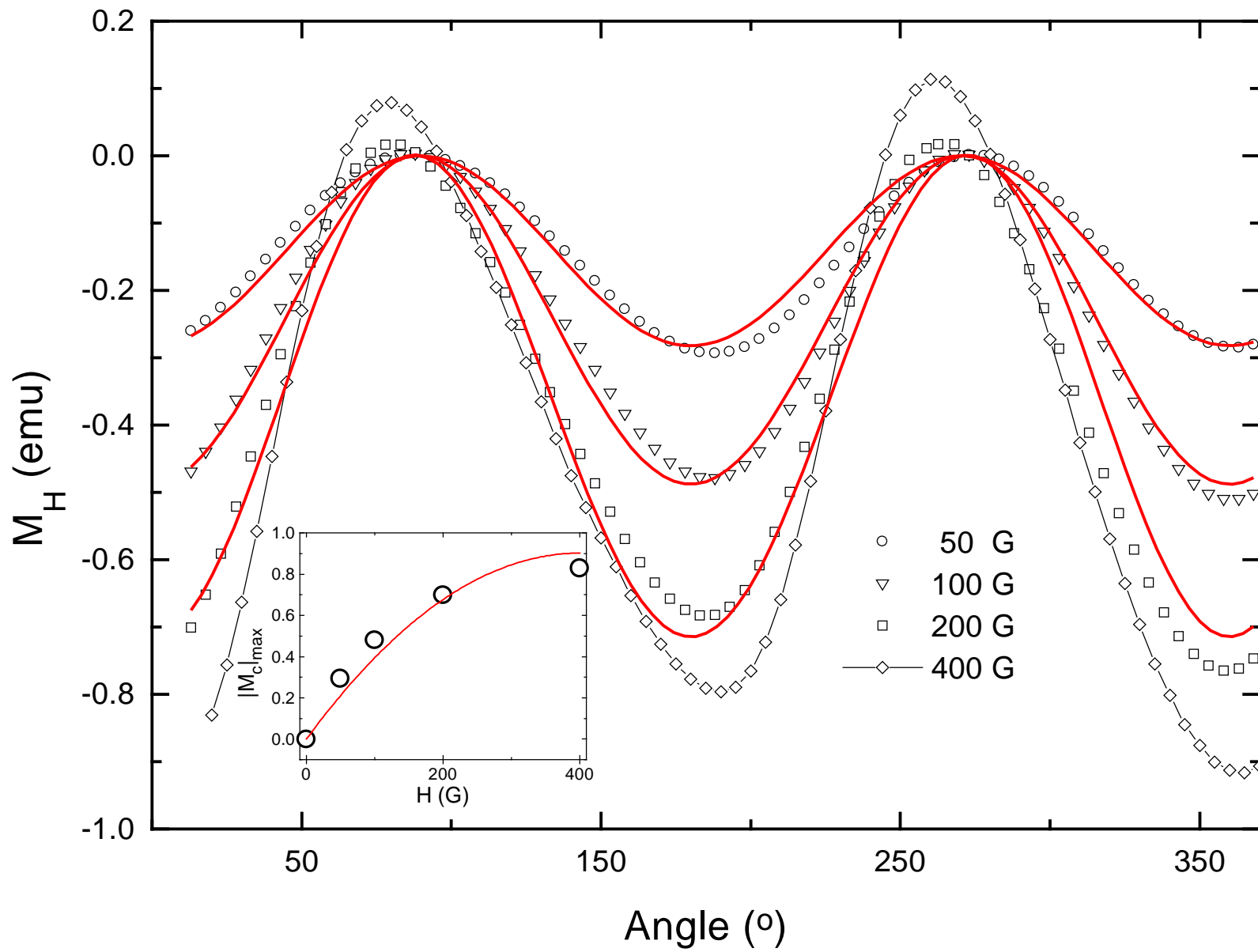
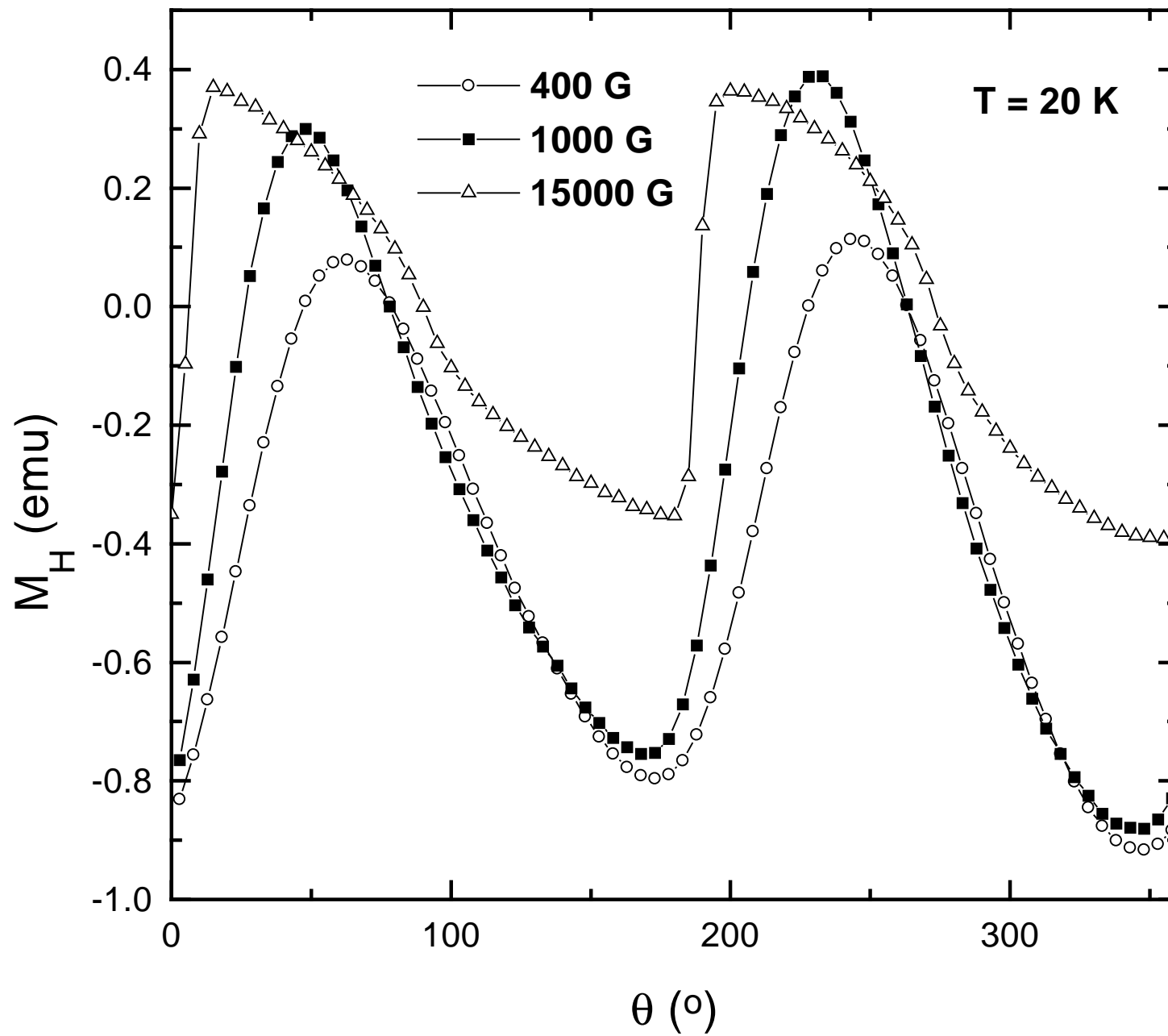


Fig.2

(Prozorov et al.)



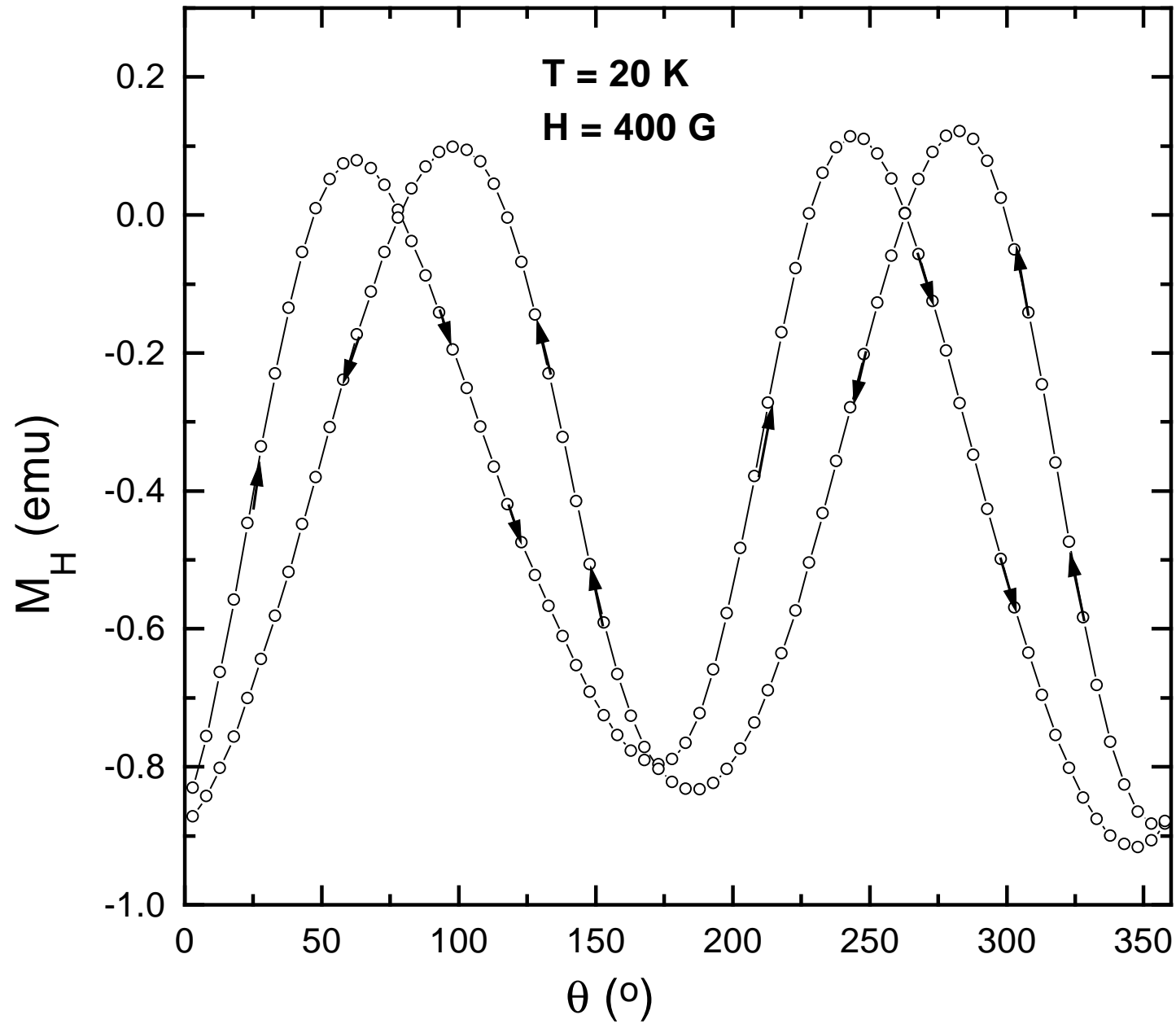


Fig. 4 (Prozorov et al.)

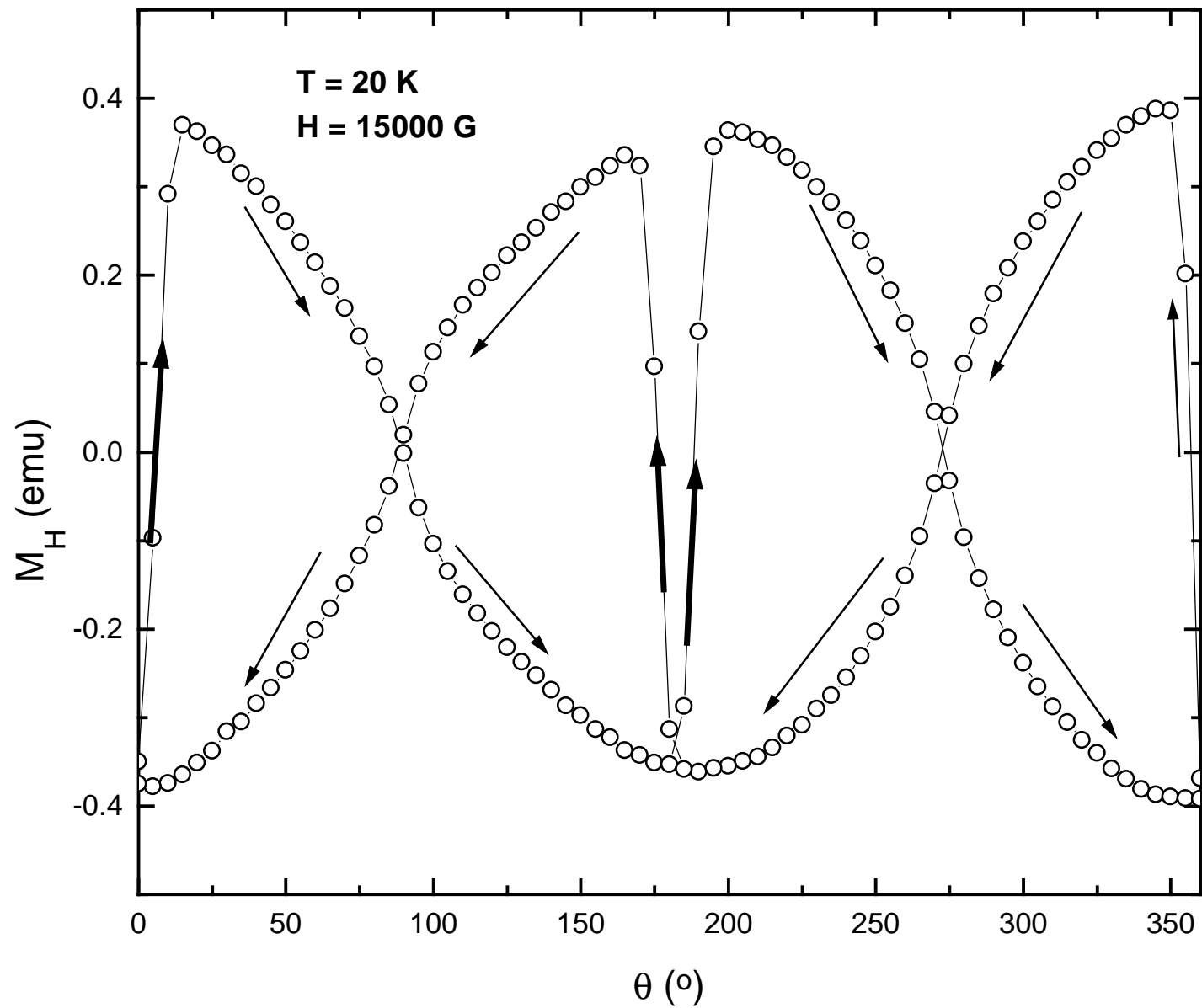


Fig. 5 (Prozorov et al.)

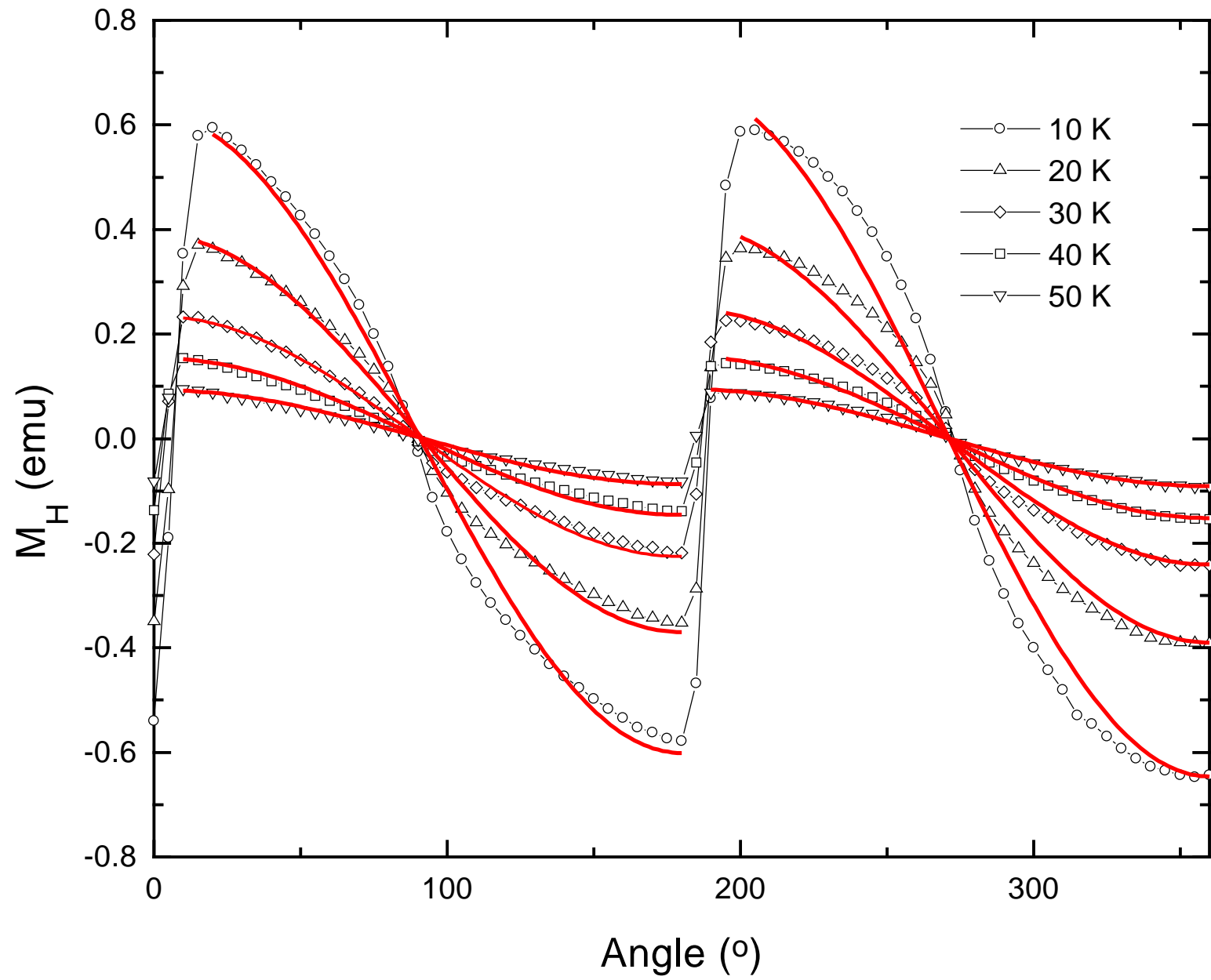


Fig.6

(Prozorov et al.)

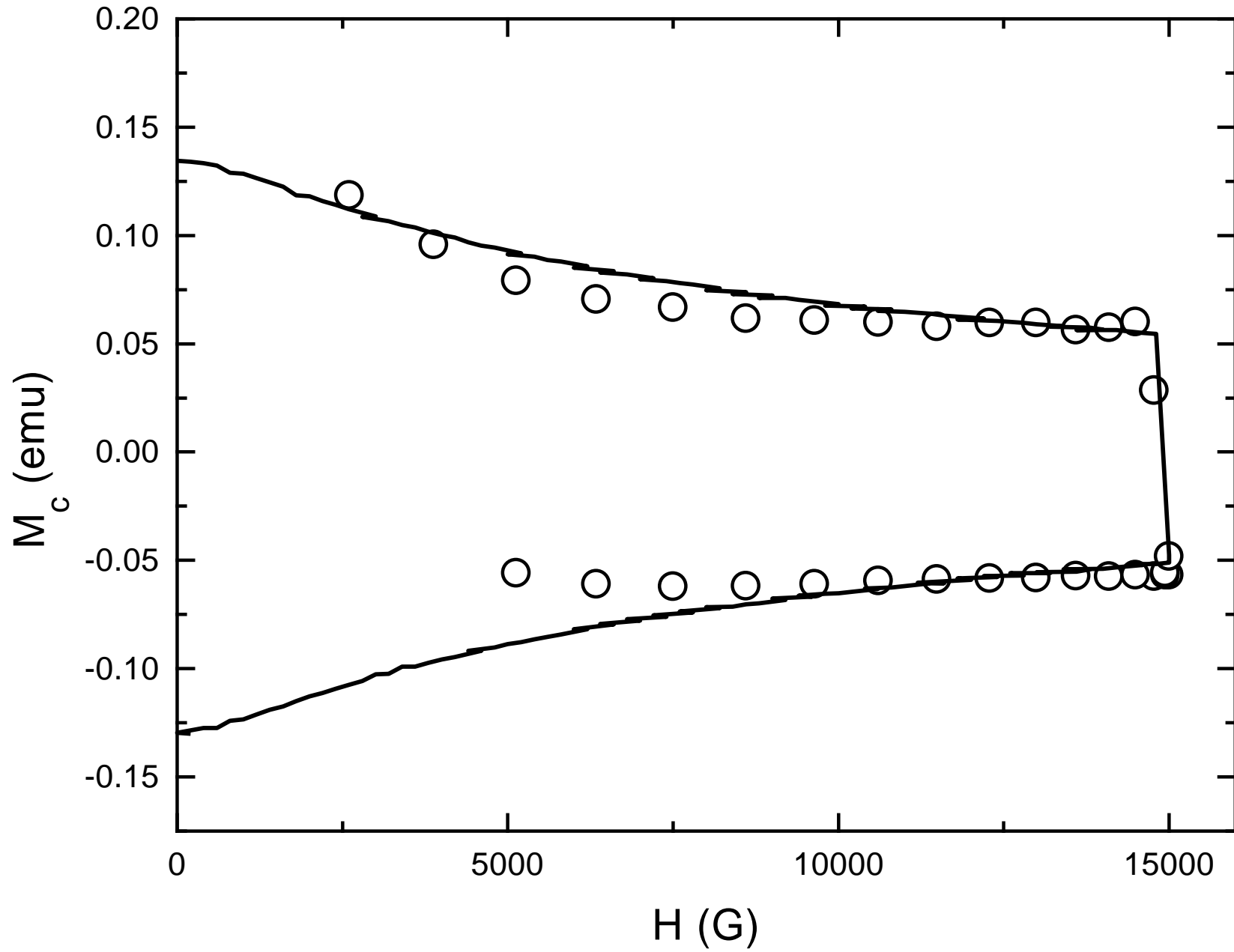


Fig. 7

(Prozorov et al.)